RASĀYAN *J. Chem.*
Vol. 18 | No. 1 |341-351| January - March | 2025
ISSN: 0974-1496 | e-ISSN: 0976-0083 | CODEN: RJCABP
http://www.rasayanjournal.com
http://www.rasayanjournal.co.in

STUDY OF 1-[4-H NITROPHENYL] PYRROLE-2-CARBALDEHYDE TO MITIGATE CORROSION OF MILD STEEL IN ACIDIC SOLUTION

Sahil Satarkar[1,✉] and R. S. Dubey[2]
Department of Chemistry, R.J. College (Autonomous), Ghatkopar (W), Mumbai-400086, India
✉Corresponding author: sahilsatarkar@gmail.com

ABSTRACT
The corrosion prevention of mild steel was studied using a synthetic pyrrole derivative, 1-[4-H nitrophenyl] pyrrole-2-carbaldehyde. The experiments involved weight reduction treatments, electrochemical analysis, and surface analysis. Corrosion inhibition was seen to increase in the presence of the studied inhibitor, and the inhibition efficiency was observed to be directly proportional to the inhibitor concentration. The tested inhibitor has a maximum inhibition efficacy of 88.67% at 600 ppm. The inhibitory efficiency decreased as the solution's temperature increased. Electrochemical investigation revealed that the examined pyrrole derivative worked as a mixed sort of inhibitor. The formed energy barrier on the metal surface was confirmed by the surface analytical techniques.
Keywords: Corrosion, Inhibition, Pyrrole, Gravimetric Analysis, Adsorption.
RASĀYAN *J. Chem.*, Vol. 18, No.1, 2025

INTRODUCTION

Mild steel is the most widely used alloy in various industries due to its mechanical qualities, chemical properties, weldability, and machinability. Mild steels are commonly used to manufacture tanks, petrochemical refinery equipment, pipes, and boilers. In mild steel, Corrosion occurs when touched with acidic liquids. Generally, hydrochloric and sulfuric acids are utilized for acid pickling steel, chemical cleaning and processing, ore production, and oil well acidification.[1-2] Metal dissolves in an acidic liquid, altering its characteristics. This could fail industrial components and systems.[3-5] Various approaches for protecting mild steel from acidic solutions have been developed, including material selection, anodic or cathodic protection, and coatings; nevertheless, the application of inhibitors is the most generally employed technique to minimize corrosion.[4,6] Most organic compounds containing heteroatoms (N, O, S, P) and pi-electrons are thought to be effective corrosion inhibitors. Inhibition occurs when pi-electrons and heteroatom electrons are adsorbed and create a protective coating on the metal surface. Adsorption can happen either physically or chemically. The chemisorption mechanism occurs when inhibitor electrons engage with the unoccupied d-orbital of iron in mild steel, whereas the physisorption process occurs when a charged inhibitor molecule interacts with the metal surface.[7-9] However, nitrogen-containing compounds are thought to be more effective in hydrochloric acid solutions.[10] The present study investigated the corrosion inhibition properties of synthesized 1-[4-H nitrophenyl] pyrrole-2-carbaldehyde. The investigation was carried out by using weight loss at room temperature and elevated temperatures, open circuit potential, potentiodynamic polarization, scanning electron microscope (SEM), and energy dispersive X-ray (EDAX) analysis.

EXPERIMENTAL

Material

Rectangular Mild steel coupons of dimensions 1 cm*3.5 cm*0.020 cm and of composition C (0.16%), Mn (0.40%), Si (0.10%), S (0.02%), P (0.013%) and iron (remaining) were employed for all the experimental analyses. The mild steel coupons were abraded using emery paper, degreased with acetone, dried in a desiccator, and then used for experimental analysis.

Inhibitor and Solution

AR grade 36% HCl solution was diluted by double distilled water to prepare the 0.1N hydrochloric acid solution. The prepared acidic solution was used in the presence of different concentrations of the studied inhibitor.

http://doi.org/10.31788/RJC.2025.1819134

Synthesis

In a 250cm^3 round-bottom flask, 2.5 cm^3 of furfural was dissolved in 100 cm^3 of ethanol. To this solution, 6.9g of 4-nitroaniline and 2 cm^3 of conc. HCl was added. The reaction mixture was heated in a water bath for two hours. After cooling, it was poured into ice-cool water with stirring. The precipitate obtained was filtered and recrystallized using a methanol and ethyl acetate mixture.[11]

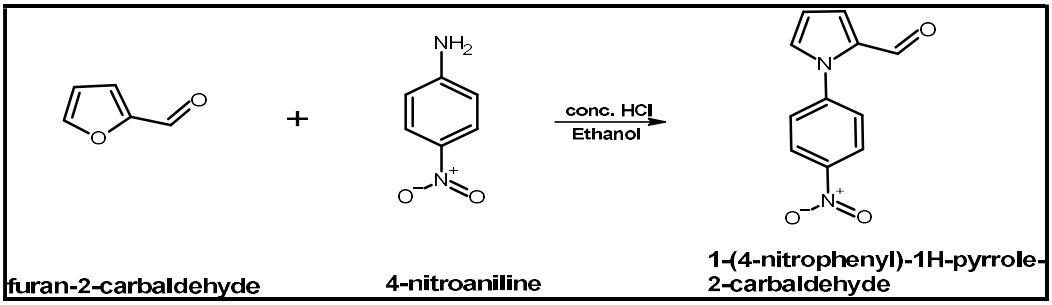

Fig.-1: Synthesis of 1-[4-H nitrophenyl] pyrrole-2-carbaldehyde

Weight Loss Analysis

The weight loss procedure was carried out in a testing tube containing 0.1N acidic solution with and without various doses of the investigated inhibitor. Six different concentrations (100 ppm to 600 ppm) were prepared. Weight loss analysis was performed at room temperature (24-hour immersion) at three higher temperatures (323K, 333K, and 343K) (one-hour immersion). The weight of mild steel coupons was measured before immersing them in their respective solutions. After their respective times, the metal coupons were washed with acetone and dried. The weight of the metal coupons was recorded, and the corrosion rate was estimated using the following equation based on the difference in weight between the mild steel coupons.

$$C.R = \frac{W}{St} \quad (1)$$

"The C.R is the corrosion rate, W is the difference in the weight of the metal coupons observed, S is the surface area of the metal coupon and t is the immersion time".

From the corrosion rate, the inhibition efficiency (%) was calculated by employing the following equation.

$$IE(\%) = \frac{C.R - C.R'}{C.R} X\ 100 \quad (2)$$

"Where C. R is the corrosion rate of the uninhibited metal surface and C. R′ Is the corrosion rate of the inhibited metal surface".

The surface coverage (θ) was obtained by using the following equation

$$\theta = \frac{C.R - C.R\prime}{C.R} \quad (3)$$

Electrochemical Analysis

The electrochemical analysis to obtain polarization curves was done by using Admiral Instruments' electrochemical measuring equipment, the Squidstat Solo 2181. The metal coupons were polished and then coated with enamel lacquer. A 1cm^2 working area was left uncovered to provide the electrical contact. The experiment was carried out in a Pyrex glass tank with three necks for electrodes. The working electrode (mild steel coupon), reference electrode (calomel electrode), and counter electrode (graphite electrode) were immersed in a three-necked flask with 100cm^3 of test fluid and connected to the device. The potentials were swept from -0.25 V to +0.25 V at a scan rate of 5 mV/s. OCP curves were recorded first, followed by polarization curves, to obtain the steady-state potential.

Surface Analytical Technique

The surface morphology of the metal surface in the presence of 600 ppm inhibitor concentration was investigated using surface analytical techniques such as SEM and EDAX.

RESULTS AND DISCUSSION

Characterization

The Perkin-Elmer 1710 spectrophotometer was used to record "The Fourier Transform Infrared Spectrum (FTIR)" in the range of 500-4000 cm^{-1} at a resolution of 2 cm^{-1} to investigate the properties of the produced

inhibitor. 1-[4-H nitrophenyl] pyrrole-2-carbaldehyde: Yield: 63.94%, Melting Point: 164°C-166°C, FTIR (KBr cm-1): 3075.77 (C-H), 2823.66 (=C-H), 1695.97 (C=O), 1622.98 (C=C), 1562.68 (NO_2), 1275.4 (C-N).

Weight Loss Analysis

Effect of Concentration

The results obtained from the weight loss analysis at different concentrations of the inhibitor are listed in Table-1. According to the data listed in Table-1, a significant decrease in the corrosion rate was observed in the presence of an inhibitor. Also, as the concentration of the inhibitor was increased, the inhibition efficiency was observed to increase. At a concentration of 600 ppm of inhibitor, the greatest inhibition efficiency was 88.67%. Further increasing the inhibitor concentration did not result in a significant change in the inhibition efficiency. Thus, it can be concluded that the 600-ppm concentration was the optimum concentration for the maximum surface coverage. The increase in the inhibition efficiency in the presence of an inhibitor indicates that the studied inhibitor has adsorbed on the mild steel surface and the adsorption increases as the concentration of the inhibitor increases due to the more availability of the inhibitor molecule to get adsorbed on the metal surface.[12]

Table-1: Weight Loss Data Obtained for Mild Steel in 0.1N HCl Solution at Different Concentrations of Pyrrole Derivative

S.No.	C (ppm)	Inhibition Efficiency (IE%)	Corrosion Rate ($mgcm^{-2}h^{-1}$)	Surface Coverage (θ)
1	0.00	-	0.220	-
2	100	47.16	0.169	0.47
3	200	66.03	0.104	0.66
4	300	77.35	0.069	0.77
5	400	83.05	0.052	0.83
6	500	86.79	0.040	0.86
7	600	88.67	0.034	0.88

Effect of Temperature

The corrosion inhibition of 1-[4-H nitrophenyl] pyrrole-2-carbaldehyde was investigated at three elevated temperatures (323K, 333K, 343K). The corrosion rate and inhibition efficiency obtained are listed in Table (2). According to the results obtained, it was observed that at higher temperatures the corrosion rate increased significantly because at higher temperatures the kinetics of anodic and cathodic reactions increased, thus increasing the metal dissolution process. Also, on increasing the solution temperature the inhibitor efficiency decreased. The efficiency decreased from 93.61% at 323K to 78.12% at 343K. This indicates, that at higher temperatures there is a decrease in the interaction between the inhibitor and the metal surface. Due to this, the adsorbed inhibitor on the metal surface gets desorbed back into the solution. Thus, forming voids on the formed protective layer on the metal surface and giving rise to pitting corrosion.[12-13]

Table-2: Weight Loss Data for Mild Steel at Three Elevated Temperatures

	Corrosion Rate ($mg\ cm^{-2}\ h^{-1}$)			Inhibition Efficiency (%)		
Concentration (ppm)	323K	33K	343K	323K	33K	343K
Blank	6.54	7.79	8.91	-	-	-
100	1.67	2.92	4.17	74.46	62.5	53.12
200	1.39	2.36	3.34	78.72	69.64	62.5
300	0.97	1.81	2.64	85.10	76.78	70.31
400	0.69	1.39	2.36	89.36	82.14	73.43
500	0.41	1.11	1.94	93.61	85.71	78.12

Activation Parameters

The effect of temperature on the mild steel surface can be best explained by using the following Arrhenius equation.

$$\ln C.R = \ln A - \frac{Ea}{RT} \quad (4)$$

Ea is the activation energy, A is the frequency factor, R is the universal gas constant and T is the absolute temperature. Activation parameter like activation energy (Ea) was calculated from the slope of the activation plot Fig.-2 and are listed in Table-3. From the data obtained, the values of activation energy were lower for uninhibited mild steel coupon and the value increased on increasing the inhibitor concentration. This indicated that more energy is required to dissolve the metal in the solution. The higher activation energy in the presence of an inhibitor indicates that the inhibitor has formed a protective film on the mild steel surface and acts as an energy barrier between the acidic solution and the mild steel surface.[12,14]

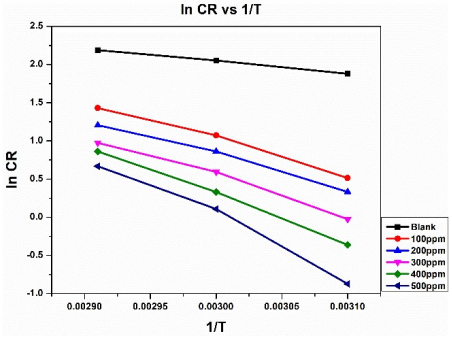

Fig.-2: Arrhenius Plot for Mild Steel Corrosion in 0.1N HCl Solution with and without Different Concentrations of 1-[4-H nitrophenyl] pyrrole-2-carbaldehyde

Table-3: Activation Parameters Data of Mild Steel in the Presence of the Studied Inhibitor

S.No.	Concentration (ppm)	R^2	Ea (kJ/mol)	ΔH (kJ/mol)	-ΔS (J/mol)	ΔG			
						303K	323K	333K	343K
1	0	0.995	14.24	10.86	196.14	70.29	74.21	76.17	78.13
2	100	0.982	42.18	37.55	124.54	75.28	77.77	79.02	80.08
3	200	0.998	40.35	35.71	131.79	75.64	78.27	79.59	80.91
4	300	0.988	46.00	41.15	117.82	76.84	79.20	80.38	81.56
5	400	0.959	55.38	50.97	90.29	78.32	80.13	81.03	81.93
6	500	0.979	70.93	64.96	50.83	80.36	81.37	81.88	82.39

The alternate form of the Arrhenius equation was used to determine the enthalpy of activation (ΔH) and entropy of activation (ΔS) as given below:

$$C.R = \frac{RT}{Nh} exp\left[\frac{\Delta S}{R}\right] exp\left[-\frac{\Delta H}{RT}\right] \quad (5)$$

(ΔH) is the enthalpy of activation, (ΔS) is the entropy of activation, h is Planks constant, R is the universal gas constant, N is Avogadro's constant, and T is the absolute temperature. Figure-3 shows the transition state graphs (ln C.R/T vs 1/T) for mild steel coupons in the presence and absence of the investigated inhibitor. The slope and y-intercept of the plot were used to derive the values of enthalpy of activation and enthalpy of entropy, which are reported in Table-3. The data showed that ΔH values were positive and increased with increasing inhibitor concentration. This implies a slower breakdown of metal in the presence of an inhibitor, which was caused by the protective coating created on the inhibitor's metal surface. The negative and growing ΔS values indicate an increase in entropy due to the formation of the activated complex.[15-19] The change in the Gibbs free energy of activation was calculated using the following equation:

$$\Delta G = \Delta H - T\Delta S \quad (6)$$

The obtained (ΔG) values are presented in Table (3). The results obtained were positive and rose in proportion to the solution's concentration and temperature. At higher temperatures, the corrosion process becomes spontaneous and the inhibitor desorbs, reducing the protective barrier on the mild steel surface. This leads to an increase in ΔG values.[20-21]

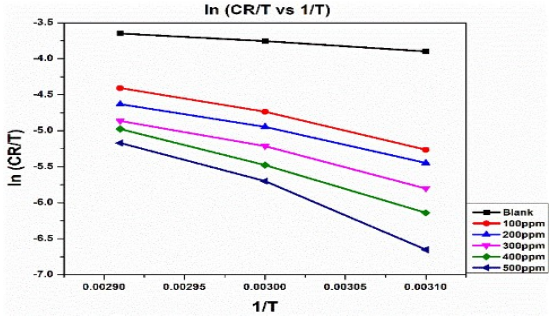

Fig.-3: Transition State Plots for the Mild Steel Coupons in the Presence and Absence of the Studied Inhibitor

Adsorption Isotherm

To understand the interaction between the mild steel surface and the inhibitor, various adsorption isotherms were studied. It was observed that the obtained data best fitted the Langmuir adsorption isotherms.

$$\frac{C}{\theta} = \frac{1}{Kads} + C \qquad (7)$$

(Kads) is the absorptive coefficient constant, C is the concentration of the inhibitor and θ Is the surface coverage? The Langmuir adsorption plots are shown in Fig.-4. From the plot, linearity was observed and the linear regression coefficient (R^2) and slope values were close to unity and are listed in Table-4. This suggests that the used inhibitor follows Langmuir adsorption isotherm and forms a uniform monolayer on the metal surface to protect it from corrosion.[22]

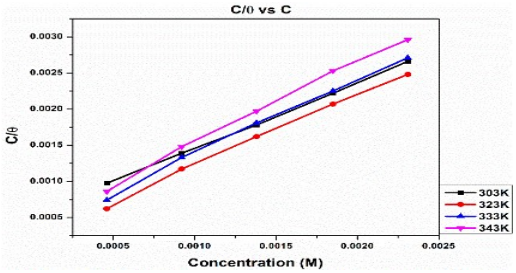

Fig.-4: Adsorption Plots of Mild Steel Coupons in Acidic Solution at Different Temperatures

The adsorption coefficient constant (K_{ads}), listed in Table-4 was calculated from the y-intercept from the plot of C/ θ vs. C. It was observed that the (K_{ads}) values decreased as the temperature was increased. The (K_{ads}) values indicate how strongly an inhibitor adheres to the metal surface. The lower (K_{ads}) values at higher temperatures indicated a weak adherence due to the dissolution of the inhibitor back into the solution.[22-23] The standard free energy of adsorption (ΔG^0_{ads}) listed in Table-4 was calculated by using Eq.(8).

$$(\Delta G^0_{ads}) = -RT \ln (55.5\ K_{ads}) \qquad (8)$$

The negative values of (ΔG^0_{ads}) suggested the spontaneous adsorption process of the used inhibitor. According to the literature, if the values of (ΔG^0_{ads}) are around -20kJ/mol, then there is an electrostatic interaction between the used inhibitor and the metal surface giving rise to a physical type of adsorption, and if the values are around or more than -40kJ/mol then an interaction between electron of inhibitor and the vacant d-orbital of the iron takes place giving rise to the chemical type of adsorption. For 1-[4-H nitrophenyl] pyrrole-2-carbaldehyde the values of (ΔG^0_{ads}) were between -29.10 kJ/mol and 33.830 kJ/mol, indicating that the used inhibitor adsorbed on the metal surface by both physical as well as chemical adsorption.[24-26]

The Vant's Hoff equation was employed to calculate the adsorption enthalpy ($\Delta H°_{ads}$) and adsorption entropy ($\Delta S°_{ads}$). The obtained values are listed in Table-4.

$$\ln K_{ads} = -\frac{\Delta H^0_{a\,ds}}{RT} + \frac{\Delta S^0_{a\,ds}}{R} + ln\frac{1}{55{\cdot}5} \qquad (9)$$

Table-4: Thermodynamic Adsorption Parameters of 1-[4-H nitrophenyl] pyrrole-2-carbaldehyde at Different Temperatures

S. No.	Temperature (K)	R^2	Slope	K_{ads}	$-\Delta G^0_{ads}$ (kJ/mol)	$\Delta H^0_{a\,ds}$ (kJ/mol)	$\Delta S^0_{a\,ds}$ (J/mol)
1	303	0.9996	0.90	1876	29.10	-26.98	20.11
2	323	0.9969	0.9977	4739	33.51		
3	333	0.9963	1.049	3174	33.44		
4	343	0.9966	1.133	2557	33.83		

From the plot of ln K_{ads} Vs 1/T Fig (5). The values of $\Delta H^0_{a\,ds}$ and $\Delta S^0_{a\,ds}$ Are calculated from the slope and the intercept respectively. The negative values of ΔH^0_{ads} The used inhibitor indicated spontaneous exothermic adsorption process which attributes lower inhibition efficiency at higher temperatures. The positive value of ΔS^0_{ads} Indicated that the entropy of the system increased during the adsorption process because of the desorption of water molecules.[25-27]

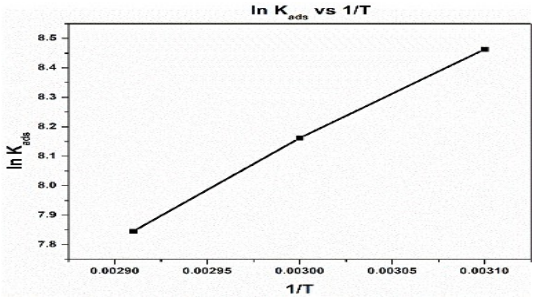

Fig.-5: Van't Hoff Plot of Mild Steel in Acidic Solution

Electrochemical Analysis

Open Circuit Potential (OCP)

The open circuit potential of mild steel in the presence and absence of the inhibitor was studied. The resultant OCP curves are shown in Fig.-6. The curves revealed that the unfettered solution's steady-state potential was more negative, whereas the inhibited solution's potential was more positive. In addition, when the inhibitor concentration grew, so did the steady potential. This demonstrated that the adsorption inhibitor on the metal surface caused a decrease in metal dissolution, shifting the working electrode potential to the anodic side. This demonstrates that the employed inhibitor was successfully adsorbed on the metal surface and established a protective coating.[28-29]

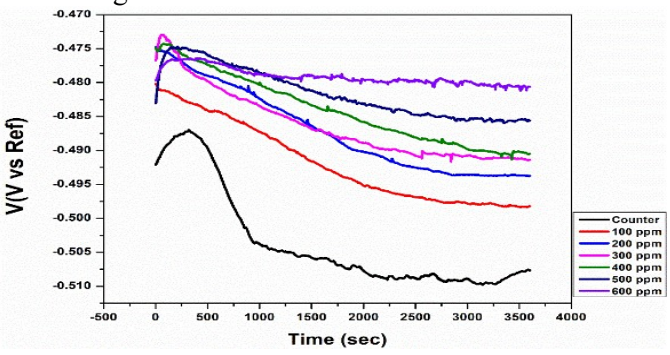

Fig.-6: OCP Curves for Mild Steel in the Acidic Solution in the Presence and Absence of the Studied Inhibitor

Potentiodynamic Polarization

Figure-7 shows the polarization curves produced in 0.1N HCl solution with varying inhibitor doses. The electrochemical parameters derived from the polarization plots are reported in Table-5. The findings revealed that as the concentration of the inhibitor grew, the corrosion current density values (icorr) declined, changing the anodic Tafel slope and cathodic Tafel slope toward lower current densities. A considerable reduction in corrosion rate was also noted. The inhibitory efficiency was computed using Eq (10), and the results are shown in Table-5.

$$IE\% = \frac{icorr - icorr}{icorr} X\ 100 \quad (10)$$

Where i_{corr} is the corrosion current densities of uninhibited mild steel and i_{corr}' is the corrosion current densities in the presence of the inhibitor.

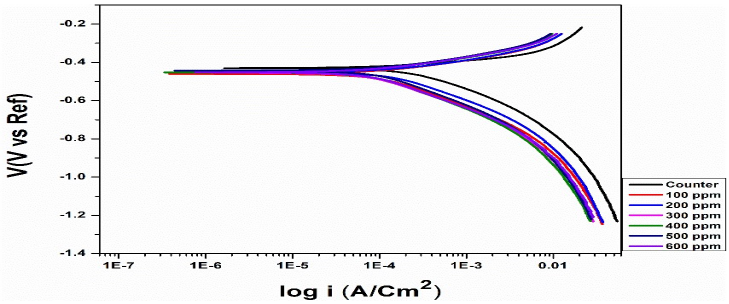

Fig.-7: Potentiodynamic Polarization Curve for Mild Steel in 0.1N HCl in the Presence and Absence of 1-[4-H Nitrophenyl] pyrrole-2-carbaldehyde

Table-5: Potentiodynamic Polarization Parameters for the Corrosion of Mild Steel In 0.1 N HCl without and with different Concentrations of 1-[4-H nitrophenyl] pyrrole-2-carbaldehyde

S.No.	Concentration (ppm)	β_a 10^{-3} (V/dec)	β_c 10^{-3} (V/dec)	i_{corr} (μA)	$-E_{corr}$ (mV)	CR (mpy)	Inhibition Efficiency (%)
1	0	81.7	223	409	434	187.15	-
2	100	91.5	222	201	459	91.80	50.85
3	200	82	182	164	454	74.86	59.90
4	300	84.3	183	107	458	49.25	73.83
5	400	70.7	176	82	452	37.50	79.95
6	500	46.6	145	64.3	436	29.43	84.27
7	600	31.9	100	37.6	445	17.22	90.80

As expected, the inhibition efficiency improved as the inhibitor concentration increased. The maximum inhibition was 90.70% at a concentration of 600 ppm. According to the literature, if the difference in Ecorr values between unfettered and inhibited solutions is greater than 85 mV, the inhibitor is classified as cathodic or anodic. In the current study, the largest difference in the Ecorr value was 25 mV, indicating that the inhibitor utilized is a mixed kind. The employed inhibitor is adsorbed on the mild steel surface, inhibiting the processes taking place on the anode and cathode. Furthermore, no changes are detected in the cathodic and anodic curves, indicating that [28-30]

Surface Analysis

Scanning Electron Microscope (SEM)

The surface morphology of the mild steel in the presence and absence of 600ppm of inhibitor in 0.1N HCl solution was investigated by using a scanning electron microscope. Figure-(8 A), depicts the SEM image of a mild steel surface before immersing it in the 0.1N acidic solution. Figure-(8 B) shows the SEM image of the mild steel surface after immersion in 0.1N acidic solution for 24 hours. Figure-(8 C) illustrates the SEM image of a mild steel surface after immersion in 0.1N acidic solution in the presence of 600 ppm inhibitor concentration for 24 hours.

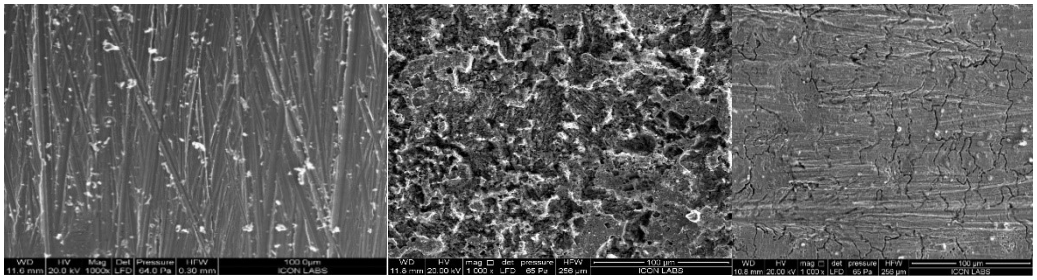

Fig.-8 A Fig.-8 B Fig.-8 C

From Fig.-(8 A), it was observed that the SEM image before immersing the mild steel in 0.1 N HCl solution had a smooth surface and there was no formation of pits or cracks, in Fig.-(8 B), pits and cracks formed on the mild steel surface. This proves that in the presence of an acidic medium, the destruction of metal takes place. A plain surface with fewer cracks was obtained in the presence of the used inhibitor. This proves that the used inhibitor has successfully adsorbed on the mild steel to protect it in an acidic medium.[31]

EDAX Analysis

The generated protective barrier on the metal surface was investigated using the EDAX analytical technique. Figure-9A displays the EDAX spectra of a mild steel surface before immersion in 0.1N acidic solution. Figure-9 B depicts the EDAX spectra of a mild steel surface after 24 hours of immersion in 0.1N acidic solution. Figure-9 C shows the EDAX spectra of a mild steel surface after 24 hours of immersion in 0.1N acidic solution with a 600-ppm inhibitor concentration. The collected EDAX data is shown in Table (6).

Table-6: EDAX Analytical Data of Mild Steel in the Presence and Absence of the Studied Inhibitor

Medium	Composition %			
	Fe	O	Cl	C
Polished (9 A)	89.9	-	-	9.0
Acidic Solution (9 B)	62.9	16.7	0.8	10.6
600 ppm of the studied inhibitor	81.6	11.9	0.1	12.9

The data obtained revealed that in the absence of mild steel, the iron content of the mild steel coupon was around 90%. When exposed to an acidic media, its concentration fell to 63%. This means that metal is being destroyed. Initially, no chlorine or oxygen content is detected, but oxide and chloride ions develop in the acidic media. In the presence of the inhibitor, the iron concentration rises to 82%, and a large amount of chlorine is removed. This shows that the inhibitor reduces metal solubility in the solution.[28,29,31]

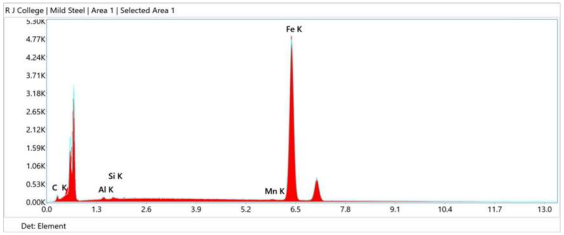

Fig.-9 A: EDAX Spectra for Polished Mild Steel

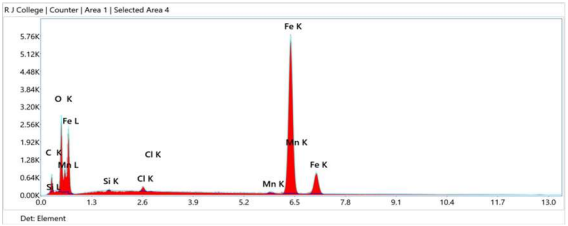

Fig.-9 B: EDAX Spectra for Mild Steel After Immersion in 0.1N Hcl Solution for 24 Hours

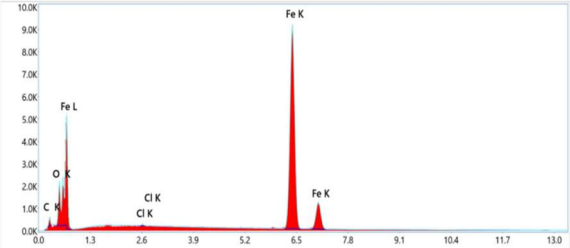

Fig.-9 C: EDAX Spectra for Mild Steel in the Presence of 600 Ppm of Studied Inhibitor

Mechanism of Inhibition

For an inhibitor to effectively adsorb on the metal surface it should contain electron-rich functional groups, heteroatoms, conjugated systems, and aromatic rings. The mechanism of corrosion inhibition of mild steel by using 1-[4-H nitrophenyl] pyrrole-2-carbaldehyde as an inhibitor can be attributed to the adsorption process. Adsorption of the organic molecule depends on the active sites and the charge present on the inhibitor molecule. In the case of used pyrrole derivate, the inhibition could have been facilitated due to the presence of electron-donating nitrogen or due to the interaction of the metal surface with the pi-electrons of the heterocyclic ring or the phenylic ring. Generally, adsorption takes place by physical adsorption process or by chemical adsorption process. The chemisorption takes place due to the interaction of electrons of heteroatoms and the iron of the metal surface. The physisorption takes place when a charged inhibitor interacts with the positively charged metal ion. Due to the presence of surface chloride ions, there is an excess amount of negative charge in the vicinity of the metal surface. This favors the adsorption of positively charged inhibitor molecules on the metal surface. The inhibition efficiency of the used inhibitor can be explained based on the interaction of polar groups like NO_2 and CHO groups with the metal surface. Also, the heteroatom and the pi-electrons present in the inhibitor can share their electrons with the vacant d-orbital of iron to give rise to the chemisorption process.[12,32]

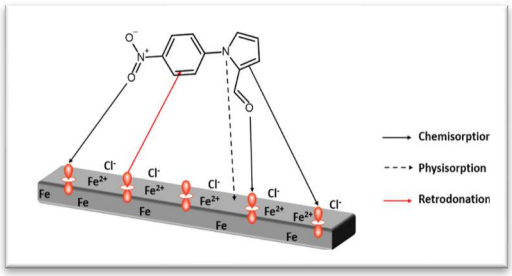

Fig.-10: Corrosion Inhibition Mechanism

CONCLUSION

The preceding study's results indicate that the inhibitor 1-[4-H nitrophenyl] pyrrole-2-carbaldehyde inhibited mild steel corrosion in 0.1N HCl solution. The weight loss analysis revealed that raising the inhibitor doses improved the inhibition efficiency. 600 ppm of concentration was determined to be the ideal concentration. As the solution temperature increased, the inhibition efficiency dropped. The adsorption of the employed inhibitor followed the Langmuir adsorption isotherm, forming a monolayer on the metal surface. The utilized inhibitor was discovered to aid in both physical and chemical adsorption processes. The electrochemical investigation revealed that the inhibitor utilized was of a mixed type. The SEM and EDAX analysis provided support for the formation of the passive film. The gravimetric and electrochemical analytical data were in good agreement.

ACKNOWLEDGMENTS

The authors are thankful to the authorities of their institutions for their encouragement and support during this research.

CONFLICT OF INTERESTS

The authors declare that there is no conflict of interest.

AUTHOR CONTRIBUTIONS

All the authors contributed significantly to this manuscript, participated in reviewing/editing, and approved the final draft for publication. The research profile of the authors can be verified from their ORCID ids, given below:

Sahil Satarkar https://orcid.org/0009-0001-3695-7029
R.S. Dubey https://orcid.org/0009-0002-3803-1075

REFERENCES

1. F. Afshari, E. R. Ghomi, M. Dinari, S. Ramakrishna, *Chemistry Select,* **8(9),** e202203231(2023), https://doi.org/10.1002/slct.202203231
2. Rekha N., *International Journal of Modern Trends in Engineering and Research* **4**, 216(2018), https://doi.org/10.21884/ijmter.2017.4405.oqrs0
3. A, A.L, *Eur. Chem. Bull.* (2023) 13354–13361
4. K. Muthamma, P. Kumari, M. Lavanya, S. A. Rao, *Journal of Bio- and Tribo-Corrosion* **7,** 10(2020), https://doi.org/10.1007/s40735-020-00439-7
5. A, S, *International Journal of ChemTech Research* **8**, 391(2014).
6. J, Jain, *Iranian Journal of Chemical Engineering,* **41**, 3365 (2021).
7. I. A. Annon, A. S. Abbas, W. K. Al-Azzawi, M. M. Hanoon, A. A. Alamiery, W. nor R. W. Isahak, A. A. H. Kadhum, *South African Journal of Chemical Engineering,* **41**, 244(2022), https://doi.org/10.1016/j.sajce.2022.06.011
8. P. Geethamani, P. K. Kasthuri, *Cogent Chemistry* **1**, 1091558(2015), https://doi.org/10.1080/23312009.2015.1091558
9. R. Talat, M. Asghar, I. Tariq, Z. Akhter, F. Liaqat, L. Nadeem, A. Haider, S. Ali, *Coatings* **12**,1701(2022), https://doi.org/10.3390/coatings12111701
10. M. E. Azhar, B. Mernari, M. Traisnel, F. Bentiss, M. Lagrenée, *Corrosion Science* **43**, 2229(2001), https://doi.org/10.1016/s0010-938x(01)00034-8
11. Shahi, M. N. Ph.D. Thesis, Synthesis of Pyrrole and Other Heterocyclic System, University of Islamabad, Pakistan (2017),
12. C. Verma, M. A. Quraishi, *Ain Shams Engineering Journal,* **7(1)**,1(2016), https://doi.org/10.1016/j.asej.2015.11.017
13. A. N, S. N. S, D. Ramakrishna, R. S, *Results in Surfaces and Interfaces,* **15**, 100209(2024), https://doi.org/10.1016/j.rsurfi.2024.100209
14. C. Verma, A. Singh, G. Pallikonda, M. Chakravarty, M. A. Quraishi, I. Bahadur, E. E. Ebenso, *Journal of Molecular Liquids,* **209**, 306(2015), https://doi.org/10.1016/j.molliq.2015.06.013
15. A. M. Ashmawy, M. A. Mostafa, A.-B. Kamal, G. a. M. Ali, M. S. A. El-Gaby, *Scientific Reports,* **13,** Article number: 18555(2023), https://doi.org/10.1038/s41598-023-45659-2
16. M. Erna, H. Herdini, D. Futra, *International Journal of Chemical Engineering,* **1,** (2019), https://doi.org/10.1155/2019/8514132
17. M. E. Azhar, B. Mernari, M. Traisnel, F. Bentiss, M. Lagrenée, *Corrosion Science,* **43**, 2229(2001), https://doi.org/10.1016/s0010-938x(01)00034-8
18. P. Raotole, R. S. Khadayte, and V. Huse, *International Journal of Creative Research Thoughts*, **10(12)**, 636(2022).
19. A. O. Okewale, O. A. Adesina, *Journal of Applied Sciences and Environmental Management,* **24**, 37(2020), https://doi.org/10.4314/jasem.v24i1.6
20. K. Raviprabha, R. S. Bhat, *Egyptian Journal of Petroleum,* **32(2)**, 1(2023), https://doi.org/10.1016/j.ejpe.2023.03.002
21. A. F. S. A. Rahiman, S. Sethumanickam, *Arabian Journal of Chemistry,* **10**, S3358(2014), https://doi.org/10.1016/j.arabjc.2014.01.016
22. N. Betti, A. A. Al-Amiery, W. K. Al-Azzawi, W. nor R. W. Isahak, *Scientific Reports,* **13,** Article number: 8979(2023), https://doi.org/10.1038/s41598-023-36064-w
23. L. A. Nnanna, K. O. Uchendu, F. O. Nwosu, U. Ihekoronye, E. P. Eti, International *Journal of Materials and Chemistry*, **4(2)**, (2023).
24. X. Zheng, M. Gong, Q. Li, L. Guo, *Scientific Reports,* **8**, Article number: 9140(2018), https://doi.org/10.1038/s41598-018-27257-9
25. D. Q. Huong, T. Duong, P. C. Nam, *ACS Omega,* **4**, 14478(2019), https://doi.org/10.1021/acsomega.9b01599
26. G. Gómez-Sánchez, O. Olivares-Xometl, P. Arellanes-Lozada, N. V. Likhanova, I. V. Lijanova, J. Arriola-Morales, V. Díaz-Jiménez, J. López-Rodríguez, *International Journal of Molecular Sciences,* **24**, 6291(2023), https://doi.org/10.3390/ijms24076291

27. A. Sehmi, H. B. Ouici, A. Guendouzi, M. Ferhat, O. Benali, F. Boudjellal, *Journal of the Electrochemical Society,* **167**, 155508(2020), https://doi.org/10.1149/1945-7111/abab25
28. P. Kamble, R. S. Dubey, Corrosion Inhibition of Mild Steel Used in Oil and Natural Gas Industries by Using 5-Phenyl tetrazole, CORCON, organized by NACE International, Gateway India Section (NIGIS) (2017).
29. D. Girase, P. Kamble and R. S. Dubey, *International Research Journal of Science and Engineering*, **Special Issue A11**, 117(2021).
30. H. Kumar, S. Sharma, R. Kumari, *Vietnam Journal of Chemistry,* **60**, 417(2022), https://doi.org/10.1002/vjch.202100166
31. N. N. Bastam, H. R. H. Atabak, F. Atabaki, M. Radvar, S. Jahangiri, *Iranian Journal of Chemistry and Chemical Engineering-International English Edition,* **39**, 113(2020), https://doi.org/10.30492/ijcce.2020.38997
32. P. Kamble, R. S. Dubey, *Journal of Scientific Research,* **65**, 55(2021), https://doi.org/10.37398/jsr.2021.650607

[RJC-9134/2024]